Int. J. Electrochem. Sci., 11 **(2016)** 4198 - 4204

International Journal of ELECTROCHEMICAL SCIENCE
www.electrochemsci.org

Short Communication

Influence of Annealing on Pt Electrocatalyst: Theoretical Approach to Estimate CO Tolerance

Andrey Tokarev, and Dmitri Bessarabov

Hydrogen Infrastructure Center of Competence (HySA Infrastructure), North-West University, Faculty of Engineering, Private Bag X6001, Potchefstroom, 2520 South Africa
*E-mail: Dmitri.Bessarabov@nwu.ac.za

Received: 31 January 2016 / *Accepted:* 7 March 2016 / *Published:* 1 April 2016

For electrocatalytic energy hydrogen systems such as fuel cell (FC) and hydrogen compression there is a demanding requirement for the hydrogen purity. There is a vast opportunity to produce hydrogen from various sources, including fossil fuels; however, in many cases such hydrogen will contain various impurities, such as CO. In our previous work we showed that annealing of a catalyst affects its CO tolerance. Using the same theoretical model for investigating CO tolerance of a catalyst, we explored how temperature of annealing affects CO poisoning of a platinum whiskerette, a nanoobject of an extended-surface support, such as 3M nanostructured thin film (NSTF), or other structures produced by, for example, glancing angle deposition (GLAD) methods, etc. Here we present results of molecular dynamic (MD) modeling of the whiskerette as a model of extended structure annealed at temperatures from 400 to 1200 K. We found that CO coverage increases with annealing temperature, that is, at high temperatures there are more deformations which lead to high CO coverage. Interestingly, we observed sharp peak of CO coverage at temperature above 1000 K. Obtained results suggest range of optimal annealing temperatures.

Keywords: CO tolerance, extended-surface support, annealing, molecular dynamics

1. INTRODUCTION

Annealing is an important process which alters physical and chemical properties of material [1-5]. It can also affect electrochemical characteristics of the material used as a catalyst. For example, Pt-Cu alloy catalyst, annealed at 800 °C and subsequently dealloyed, showed higher activity than those annealed at 600 °C and 950 °C [6]. It can be explained by annealing-structure-activity connection: higher annealing temperature results in more compressed alloy structure, that in turn affects its activity

doi: 10.20964/1104311

[7]. In this work we used such connection in a slightly modified form: annealing-(surface structure)-activity to investigate effect of annealing on CO tolerance.

CO poisoning of a catalyst is one of the major problems in hydrogen and fuel cell industry [8-11]. As to our knowledge, relation between annealing and CO poisoning was not investigated so far. The intermediate link, that connects both processes, can be surface defects. It is known that annealing creates defects in the material [12]. In particular, it can be used to enhance conductivity and ferromagnetism in semiconductors [13]. On the other hand, as it was shown [14-17], surface defects enhance CO adsorption. Combination of two phenomena gives annealing - defects - CO adsorption relationship that we examine in the article.

Another question, we explored in the work, is what is the optimal annealing temperature. If the temperature is too high, functional characteristics of material can be reduced: for example, nanoobjects can agglomerate [18-20]. If it is too low, no desired structural changes happen. There is a need for a model capable of predicting such favorable temperature, at which annealing occurs without unwanted side effects. In this work such attempt was made.

The article is a continuation of our previous work [16] in which we studied dependence of CO tolerance on structural and surface defects, such as contraction and stretching, edges and vertices of 111 and 100 platinum and Pt_2Ru slabs. In this modeling we applied those results of quantum-chemical calculations to investigate influence of annealing temperature on CO tolerance and structural properties of a platinum whiskerette. It is important to underline that although here we considered a whiskerette, the proposed model is applied to any other nanoobject.

2. METHODS OF CALCULATIONS

Molecular dynamics (MD) calculations were performed in GULP software package [21], with NVT ensemble, using Sutton-Chen potentials [22]. Geometrical shape of the whiskerette is described in details in work of Gancs et al. [23]. It consists of a tilted pillar (base) with the square-truncated pyramids preserved on top (Fig. 1). The initial platinum whiskerette, before simulation, had sizes of a base, *length* × *width* × *height*, equal to 25 Å × 25 Å × 53 Å, and a base to top ratio of pyramid equal to ≈3, as described in literature [23]. Overall, the whiskerette consisted of 2271 atoms. The initial crystal structure was the set up to bulk structure.

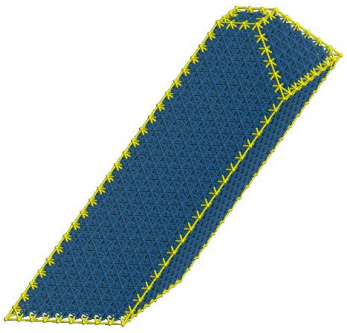

Figure 1. Initial platinum whiskerette cut from bulk. For better representation edges are marked in yellow

Annealing was performed in the range of temperatures from 400 K to 1200 K with 100 K interval with the heating and cooling rate of 0.05 K / step, and the step was equal to 1 fs. The equilibration time (to equilibrate potential and kinetic energy distribution) was 3 ps. The whiskerette was held 10 ps at the elevated temperature. Calculated CO coverage was averaged over 10 ps at the fixed temperatures: elevated and room temperature (298 K).

To compute solvent accessible surface area (ASA) we used slightly modified code (to speed up performance) by Bosco Ho [24] which implements numeric algorithm by Shrake and Rupley [25]. In particular, calculation time was reduced from quadratic $O(n^2)$ to linear $O(n)$ (where n is the number of atoms) by hashing of atoms into disjoint space cubes to speed up the search for neighboring atoms. Bottom atoms of the whiskerette were excluded from ASA calculation as not reachable to CO molecules.

3. RESULTS AND DISCUSSION

3.1. Model description

Realistic description of CO coverage should take into account not only adsorption energy, but applied temperature and surface area accessible by CO molecule as well, as accessible surface area proportionally increases chances of molecule to be adsorbed. For this purpose, a theoretical model must include both temperature and accessible surface. A Boltzmann distribution was used to calculate probabilities of CO adsorption as a function of the adsorption energy. The last one depends on the local deformation of catalyst accessible surface and temperature. As a result, probability of CO molecule adsorption at the i-th atom is given by the formula:

$$P_i(CO) = \frac{S_i}{Z} \exp\left(\frac{-E_i}{kT}\right) \qquad (1)$$

where S_i and E_i are accessible surface area and adsorption energy at temperature T of CO molecule at the i-th atom respectively, Z is a partition function, and k is the Boltzmann constant.

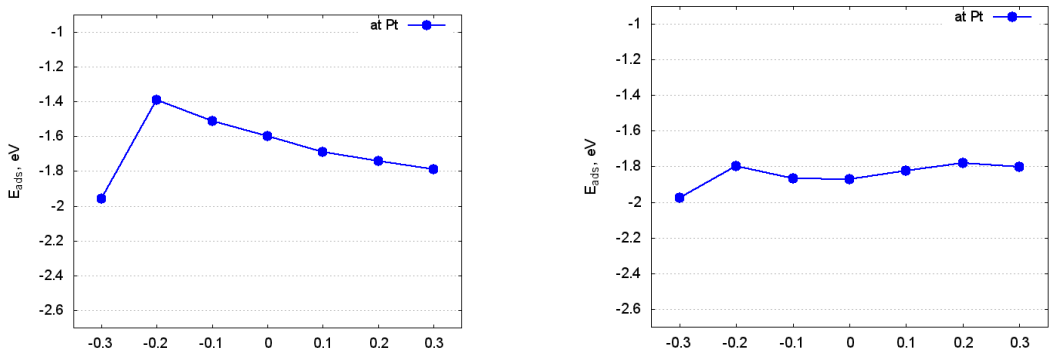

Figure 2. CO adsorption on deformed 111 and 100 platinum slabs. Negative and positive abscissa values represent contraction and stretching respectively.

To compare CO coverages of the whiskerette at different elevated temperatures, we used a room temperature value (298 K) in the formula (1). In this way, CO coverage of heated whiskerette can be considered as CO coverage of the whiskerette instantly cooled down to room temperature with the structure at the elevated temperature. Such approach, based on Boltzmann distribution, explicitly takes into account results of quantum-chemical calculations. Thus, it combines scale of molecular dynamics with precision of quantum chemistry.

Quantum-chemical calculations, that correlate surface defects with CO adsorption energy (Fig. 2), were taken from our previous work [16]. Figure 2 shows that adsorption curve depending on lattice deformation (contraction-stretching: negative and positive abscissa values represent contraction and stretching respectively) at 111 slab is decaying, while at 100 slab it is oscillating around -1.8 eV. In both cases at contraction more than -0.3/-0.2 Å surface reconstruction occurs: platinum aggregates to the surface, and surface degrades. At other type of defects, edge and vertex, CO adsorption energies are -1.9 eV and -2 eV respectively. Thus CO adsorption energy increases along the row of adsorption surface sites at 111 slab, 100 slab, edge, vertex.

To compute probability of CO adsorption, according to formula (1), the following calculation scheme was used (Fig. 3). Firstly, accessible surface area and averaged distance were computed. Then value of surface area defines type of the surface: it increases along the row of plane, edge, vertex. Averaged distance determines deformation: how stretched or contracted is local surface. Both surface area and deformation allow to calculate adsorption energy, which, in turn, with ASA give the CO adsorption probability P_i at i-th atom. Summation over all atoms of the whiskerette gives total probability of CO adsorption P_T.

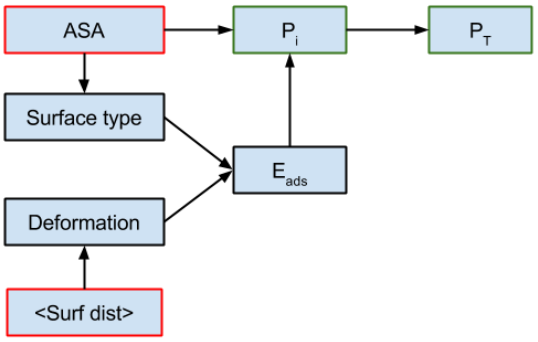

Figure 3. CO adsorption on deformed 111 and 100 platinum slabs. Negative and positive abscissa values represent contraction and stretching respectively.

One possible extension of our model is to combine it with the theoretical model that statistically predicts growth of metallic whiskers [26]. Such approach would allow to simulate effect of annealing on whiskerette growth and whiskerette catalytic activity, taking into account distribution of whiskerettes by their parameters (such as size, density etc.).

3.2. Model application to whiskerette annealing

Figure 4 presents results of MD simulations of the whiskerette annealing at temperatures from 400 K to 1200 K. It is seen that starting from around 500 K CO coverage increases with annealing temperature. The found initiation temperature is slightly lower than experimentally observed 300 C / 573 K [27]. That can be attributed to smaller size of the modeled whiskerette: whiskerette diameter is 25 Å in our modeling vs 50 Å in the experiment.

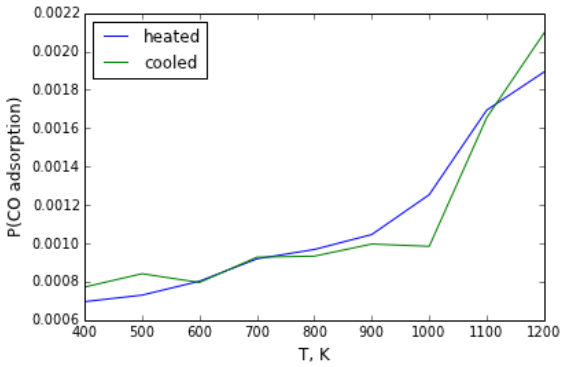

Figure 4. CO coverage probability density of the whiskerette depending on temperature of annealing. Blue curve represents coverage at annealed temperature, and green one represents coverage after cooling down to room temperature.

In the light of the proposed annealing - defects - CO adsorption relationship, such steep dependence means that at high temperatures there are more deformations which lead to high CO coverage. Indeed, Figure 5 illustrates distribution of surface type of the whiskerette at 1200 K: as it is seen, lot of defects as vertices and edges appear on the plane surface at high temperature. This observation is in line with experimental data: annealing eliminates or reduces growth of tin whiskers [28]. In a point of fact, for whiskers growth regular crystal structure of metal at micro-level is required [26], but our calculations show that annealing disturbs regularity of the crystal lattice [16].

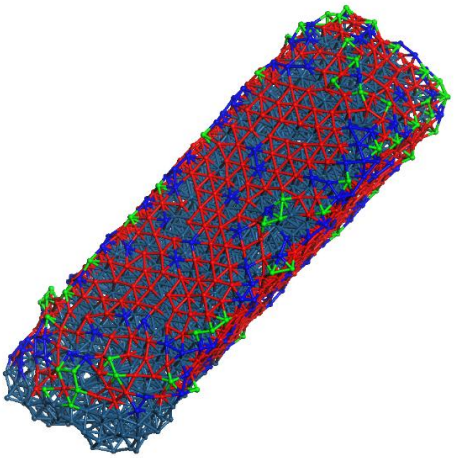

Figure 5. Map of the whiskerette surface at 1200 K. Red color represents plane sites, blue and green represent for edge-like and vertex-like sites respectively. Type of the surface is determined by accessible area as described in section *Model description*.

After cooling down to room temperature CO coverage does not return to the initial value (Fig. 4). One can say that the system has memory (in a sense of preserving structural changes). Moreover, annealing above 1000 K greatly increases CO coverage (decreases CO tolerance) at room temperature. It creates a window of annealing temperatures from 500 K to about 1000 K where annealing does not lead to a significant leap of CO coverage.

In the experimental work by Vliet et al. [27], it was shown that annealing transforms corrugated surface of a whisker, consisting of closely-packed whiskerettes, to the smooth homogeneous surface structure. In contrast, in our model we considered an isolated whiskerette. Therefore, our model does not describe collective transformation of whiskerettes and their interaction caused by heat treatment.

4. CONCLUSIONS

New model was developed to describe effect of annealing (or heat treatment in general) on CO tolerance (or catalytic and structural properties in general) of whiskerettes. Also it is widely applicable to any other nanoobjects.

We found that heating enhances CO adsorption by increasing number of surface defects. When cooled down, CO coverage does not return to the initial unaffected value, it becomes slightly larger. Moreover, annealing above 1000 K drastically boosts CO coverage, suggesting there is a window of "opportunities": annealing below 500 K does not lead to structural changes, whereas annealing above 1000 K leads to undesired raise of CO adsorption.

ACKNOWLEDGMENTS
Department of Science and Technology (DST) for funding through HySA program, as well National Research Foundation (NRF) of South Africa (NRF grant 85309). This paper was presented at the International Symposium of Electrocatalysis, Canada on October 26 - 29, 2014.

References

1. F.J. Humphreys, M. Hatherly. Recrystallization and related annealing phenomena, *Elsevier Ltd.*, (2004).
2. A. Malesevic, H. Chen, T. Hauffman, A. Vanhulsel, H. Terryn, C. van Haesendonck, *Nanotechnology*, 18 (2007) 455602.
3. G.P. Veronese, R. Rizzoli, R. Angelucci, M. Cuffiani, L. Malferrari, A. Montanari, F. Odorici, *Physica E: Low-dimensional Systems and Nanostructures*, 37 (2007) 21.
4. H. Pan, Y. Liu, M. Gao, Y. Zhu, Y. Lei, Q. Wang, *International Journal of Hydrogen Energy*, 28 (2003) 113.
5. Y.W. Tseng, F.Y. Hung, T.S. Lui, M.Y. Chen, H.W. Hsueh, *Microelectronics Reliability*, 55 (2015) 1256.
6. S. Koh, P. Strasser, *Journal of the American Chemical Society* 129 (2007) 12624.
7. P. Strasser, S. Koh, T. Anniyev, J. Greeley, K. More, C. Yu, Z. Liu, S. Kaya, D. Nordlund, H. Ogasawara, M.F. Toney, A. Nilsson, *Nature Chemistry* 2 (2010) 454.

8. Q. Li, R. He, J. Gao, J.O. Jensen, N.J. Bjerrum, *Journal of The Electrochemical Society*, 150 (2003) A1599.
9. X. Cheng, Z. Shi, N. Glass, Z. Lu, Z. Jiujun, S. Datong, Z. Liu, W. Haijiang, S, Jun. *Journal of Power Sources*, 165 (2007) 739.
10. M. Taguchi, Y. Kametani, H. Takahashi, *Materials Transactions*, 56 (2015) 353.
11. W. Shi, B. Yi, M. Hou, Z. Shao, *International Journal of Hydrogen Energy*, 32 (2007) 4412.
12. W.M. Lomer, A.H. Cottrell, *Philosophical Magazine Series*, 46 (1955) 711.
13. S.J. Potashnik, K.C. Ku, S.H. Chun, J.J. Berry, N. Samarth, P. Schiffer, *Applied Physics Letters*, 79 (2001) 1495.
14. K.J.J. Mayrhofer, M. Arenz, B.B. Blizanac, V. Stamenkovic, P.N. Ross, N.M. Markovic, *Electrochimica Acta*, 50 (2005) 5144.
15. N.P. Lebedeva, M.T.M. Koper, J.M. Feliu, R.A. van Santen, *The Journal of Physical Chemistry B*, 106 (2002) 12938.
16. A. Tokarev, D.G. Bessarabov, *International Journal of Hydrogen Energy*, 39 (2014) 7805 (2014).
17. M. Setvin, M. Buchholz, W. Hou, C. Zhang, B. Stöger, J. Hulva, T. Simschitz, X. Shi, J. Pavelec, G.S. Parkinson, M. Xu, Y. Wang, M. Schmid, C. Wöll, A. Selloni, U. Diebold, *The Journal of Physical Chemistry C*, 119 (2015) 21044.
18. J. Li, X. Liang, D.M. King, Y.B. Jiang, A.W. Weimer, *Applied Catalysis B: Environmental*, 97 (2010) 220.
19. T. Thomson, S.L. Lee, M.F. Toney, C.D. Dewhurst, F.Y. Ogrin, C.J. Oates, S. Sun, *Physical Review B*, 72 (2005) 064441.
20. D. Babonneau, G. Abadias, J. Toudert, T. Girardeau, E. Fonda, J.S. Micha, F. Petroff, *Journal of Physics: Condensed Matter*, 20 (2008) 035218.
21. J.D. Gale, A.L. Rohl, *Molecular Simulation*, 29 (2003) 291.
22. A.P. Sutton, J. Chen, *Philosophical Magazine Letters*, 61 (1990) 139.
23. L. Gancs, T. Kobayashi, M.K. Debe, R. Atanasoski, A. Wieckowski, *Chemistry of Materials*, 20 (2008) 2444.
24. B.K. Ho, F. Gruswitz, *BMC Structural Biology*, 8 (2008) 49
25. A. Shrake, J.A. Rupley, *Journal of Molecular Biology*, 79 (1973) 351.
26. V.G. Karpov, *Physical Review Applied*, 1 (2014) 044001.
27. D.F. van der Vliet, C. Wang, D. Tripkovic, D. Strmcnik, X.F. Zhang, M.K. Debe, R.T. Atanasoski, N.M. Markovic, V.R. Stamenkovic, *Nature Materials*, 11 (2012) 1051.
28. G.T. Galyon, Annotated tin whisker bibliography and anthology (2003); (http://thor.inemi.org/webdownload/newsroom/TW_biblio-July03.pdf)